LETTERS

Fullerenes from aromatic precursors by surface-catalysed cyclodehydrogenation

Gonzalo Otero[1]*, Giulio Biddau[2]*, Carlos Sánchez-Sánchez[1], Renaud Caillard[1], María F. López[1], Celia Rogero[3], F. Javier Palomares[1], Noemí Cabello[4], Miguel A. Basanta[2], José Ortega[2], Javier Méndez[1], Antonio M. Echavarren[4], Rubén Pérez[2], Berta Gómez-Lor[1] & José A. Martín-Gago[1,3]

Graphite vaporization provides an uncontrolled yet efficient means of producing fullerene molecules. However, some fullerene derivatives or unusual fullerene species might only be accessible through rational and controlled synthesis methods. Recently, such an approach has been used[1] to produce isolable amounts of the fullerene C_{60} from commercially available starting materials. But the overall process required 11 steps to generate a suitable polycyclic aromatic precursor molecule, which was then dehydrogenated in the gas phase with a yield of only about one per cent. Here we report the formation of C_{60} and the triazafullerene $C_{57}N_3$ from aromatic precursors using a highly efficient surface-catalysed cyclodehydrogenation process. We find that after deposition onto a platinum (111) surface and heating to 750 K, the precursors are transformed into the corresponding fullerene and triazafullerene molecules with about 100 per cent yield. We expect that this approach will allow the production of a range of other fullerenes and heterofullerenes[2,3], once suitable precursors are available. Also, if the process is carried out in an atmosphere containing guest species, it might even allow the encapsulation of atoms or small molecules to form endohedral fullerenes[4,5].

The surface-catalysed cyclodehydrogenation process we use to transform complex organic polyaromatic precursors of suitable topology into targeted fullerene species is sketched in Fig. 1 (see also Supplementary Fig. 1). Through vacuum thermal evaporation, we first deposit the precursor ($C_{57}H_{33}N_3$ (**1**) in the case of triazafullerene and $C_{60}H_{30}$ (**2**) in the case of fullerene) on a catalytically active metal surface. Subsequent annealing of the sample at 750 K induces a surface reaction that produces the corresponding closed molecule.

The syntheses of the planar precursors used in this work follow a previously published methodology[6–8] (see also Supplementary Information, section 1.1). Their molecular structures are optimized using two different *ab initio* total-energy methods[9,10] (Supplementary Information, Section 1.2); Fig. 1a shows a ball-and-stick model of the optimized geometry we obtain for **1**. Compounds **1** and **2** are markedly twisted, with each of the three lobes adopting a helical shape because steric congestion of their bay positions forces the outer aromatic ring of each lobe to flip up with respect to the plane of the central ring. The twisted conformation can be described by the distance the most external carbon atom is placed above the plane of the central aromatic ring (Δz), and by the twisting angle of each molecular branch. These values are respectively found to be 0.08 nm and 20.5° for **1** and 0.09 nm and 30.5° for **2**.

We have probed the cyclodehydrogenation process using scanning tunnelling microscopy (STM), X-ray photoemission spectroscopy

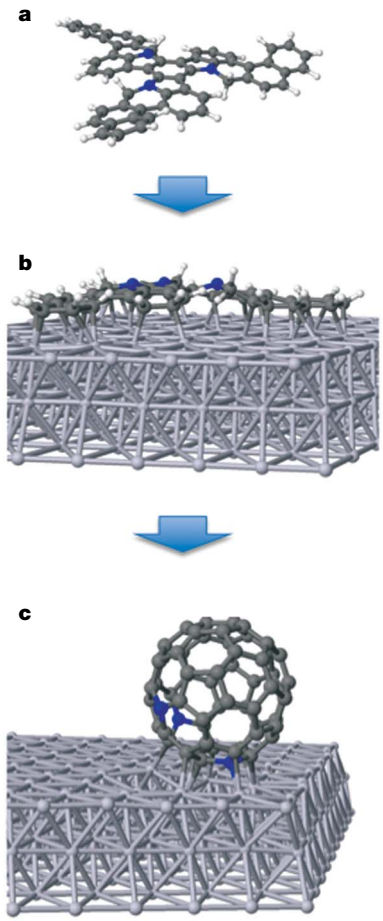

Figure 1 | Optimized geometrical structure of the $C_{57}H_{33}N_3$ molecule at the different stages of the process. a, Representation of the optimized molecular structure of the $C_{57}H_{33}N_3$ molecule. The wings of the molecule display a noticeable helicoidal twist. **b**, The same molecule adsorbed at room temperature (300 K) on the platinum (111) surface. The final relaxed configuration strongly depends on the adsorption site. The structure shown corresponds to one of the most energetically favourable sites, where the interaction with the metal substrate removes the twist and favours a markedly planar configuration for the molecule. **c**, The optimized structure for the $C_{57}N_3$ triazafullerene formed after the cyclodehydrogenation process at 750 K. Blue balls represent the nitrogen atoms in the structure.

[1]Instituto de Ciencia de Materiales de Madrid (CSIC), Cantoblanco, 28049 Madrid, Spain. [2]Departamento de Física Teórica de la Materia Condensada, Universidad Autónoma de Madrid, 28049 Madrid, Spain. [3]Centro de Astrobiología (CSIC-INTA), Carretera de Torrejón a Ajalvir, km 4, 28850 Torrejón de Ardoz, Madrid, Spain. [4]Institute of Chemical Research of Catalonia (ICIQ), Avinguda Països Catalans 16, 43007 Tarragona, Spain.
*These authors contributed equally to this work.

(XPS) and thermal programmed desorption (TPD) in an ultrahigh vacuum (UHV) environment. Figure 2a shows an STM image of **1** deposited on a platinum (111) surface with the ball-and-stick model of the adsorbed molecule superimposed. The size and topology of the STM image, with three wings characterizing the molecular shape, confirm that the molecules do not fragment, but retain their planar structure upon adsorption. A more intense protrusion (lobe) is imaged in each of the wings. These lobes are not centred; rather, their positions correspond to those of the hexagonal external rings, as can be seen by comparing the superimposed molecule with the STM image in Fig. 2a.

In a first approximation, we might speculate that the lobes correspond to the molecular orbitals of the free molecule. However, the detailed relaxed geometry is far from that of the isolated molecule: our *ab initio* calculations on a large 10×10 unit cell show that the interaction with the platinum surface is strong enough to deform the structure of the molecule. The competition between the π bonding of the rings with the surface and the energetic costs of the sterically induced molecular deformations results in a very complicated energy landscape, with barriers between local minima determined by the adsorption geometry. The general trend is a reduction of the molecular buckling (for example, Δz is reduced from 0.08 nm to 0.02 nm for **1**) as the molecular wings approach the surface to maximize the number of bonds with the surface (see also the relaxed configuration shown in Fig. 1b). The effect brings the hydrogen atoms on the wings closer to the surface, and thus plays an important role in the temperature-induced fullerene formation by surface-catalysed dehydrogenation. The strong molecule–surface interaction suggested by the calculations can also explain why we fail to observe long-range ordering of adsorbed molecules or preferential adsorption at step edges (which would require mobility of the molecule on the platinum surface). Similarly, the observation that in some imaged molecules the different lobes have different apparent heights is consistent with our calculations, which indicate that the final molecular geometry strongly depends on the adsorption site.

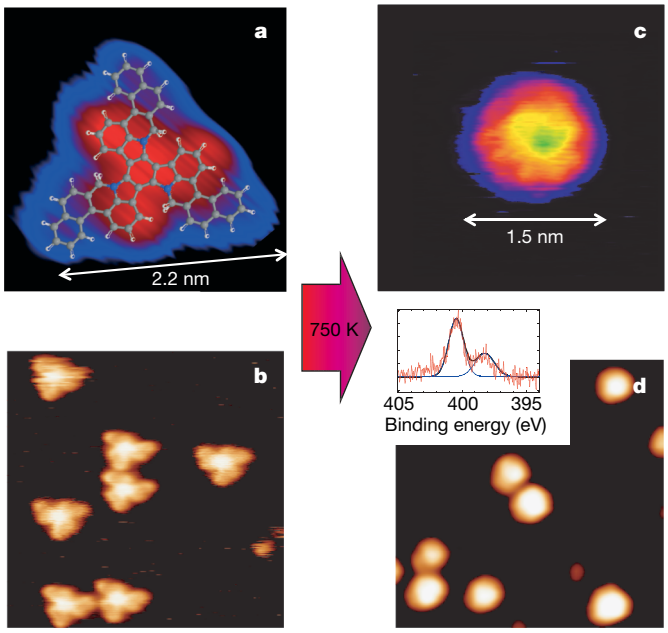

Figure 2 | STM images of the cyclization process. a, The $C_{57}H_{33}N_3$ molecule deposited on the platinum (111) surface, with the atomic structure superimposed following the calculations. **b**, $10 \times 10\ nm^2$ image of the platinum (111) surface after evaporation of about 0.2 monolayers of $C_{57}H_{33}N_3$ molecules. **c**, An isolated $C_{57}N_3$ molecule obtained after annealing the surface at 750 K. The cyclization process is inferred from the appearance of different molecular orbitals and changes in the shape and size of the imaged molecule. **d**, $10 \times 10\ nm^2$ image of the surface shown in **b**, but after annealing at 750 K. Inset, XPS spectrum of about 0.8 monolayers of $C_{57}H_{33}N_3$ molecules after annealing at 750 K. The best-fit curve of the spectrum, together with the different components used in the fit, is also shown.

As deposited on the platinum (111) surface (Fig. 2a), the heteropolyarene **1** (and similarly the polyarene **2**) presents a total apparent height in the STM images of about 0.14 nm, with no significant dependence on bias voltage. The triangular base length of the molecule is about 2.2 nm. Upon annealing the sample at 750 K, a surface reaction takes place and the triangular molecules imaged on the surface transform into round molecules with an apparent height of about 0.38 nm and a diameter of 1.5 nm (Fig. 2c). Evaporation of commercial C_{60} on a platinum surface and imaging under the same experimental conditions results in very similar STM images for the adsorbed fullerenes (Supplementary Fig. 2). A height of about 0.4 nm and a diameter of about 1.35 nm have been reported for C_{60} deposited on a platinum (110) surface[11], and a height of about 0.31 nm for C_{60} deposited on a palladium (110) surface[12]. In both these cases, the low height appears after surface annealing and suggests strong bonding of the molecule to the surface, in agreement with suggestions that the interaction of a fullerene with a platinum surface is strongly covalent and that the molecule tries to maximize the number of surface bonds[13]. We also note that the molecular orbitals visible in the STM images are similar to those reported for C_{60} on platinum[14], silicon[15] and gold[16] surfaces and are fairly well reproduced by our calculations (Supplementary Information, section 2.2); they might thus be considered as a indicator of fullerene formation.

The cyclization process shows efficiency close to 100%; that is, all the adsorbed molecules are transformed into fullerenes (Supplementary Information, section 2.3). This is illustrated by the images in Figs 2b, d of the surface covered with about 0.2 monolayers of precursor before and after annealing, respectively: the molecular coverage does not change as a result of the temperature-induced reaction, with all of the triangular molecules converted into round fullerenes.

Further evidence for the thermally induced cyclization of **1** is provided by XPS spectra of the surface covered with about 0.8 monolayers of precursor (Fig. 2d inset). Even thought this corresponds to a nitrogen coverage of only about 0.04 monolayers with respect to the platinum surface, weak emission from the nitrogen 1*s* core level is detected and confirms that after annealing, nitrogen is present on the surface (and is presumably associated with the unique topographic STM surface features, the fullerene molecules). Information on the chemical state of the nitrogen atoms is obtained from a core-level line-shape analysis of the nitrogen 1*s* spectrum, with its two peaks. The binding energy of the main peak at 400.6 eV corresponds to substitutional nitrogen in a graphite sheet, as reported for nitrogen bonded to carbon atoms in sp^2 hybridization[17]. This is the nitrogen coordination in the triazafullerene we have formed. The binding energy of the small peak at 398.2 eV is related to PtN_x compounds, in which nitrogen is chemisorbed[18]. Therefore, the smaller peak can be attributed to nitrogen atoms in the fullerene cage interacting with the platinum surface. This core-level analysis thus indicates that about one-third of the nitrogen atoms of the triazafullerene $C_{57}N_3$ interact with the surface, whereas, as a consequence of the heterofullerene curvature (see Fig. 1c), the rest are not in contact with the surface. The XPS observations also confirm the 100% efficiency of the cyclodehydrogenation process because the nitrogen 1*s* intensity does not change significantly after annealing, indicating that all the deposited molecules have cyclized (Supplementary Information, section 2.5).

The strong covalent interaction between the precursor molecules and the platinum surface appears important for the efficiency of the process. To test this idea, we evaporate **1** and **2** on a gold (111) surface that is quite inert and does not promote the cyclization reaction. The molecule–substrate interaction is negligible on this surface and, consequently, molecular diffusion at room temperature is enhanced, inhibiting the dehydrogenation process. The cyclization efficiency is reduced in this case to about 1%, with most of the molecules

decomposing. In the test with polyarene **2**, the few isolated C_{60} molecules that are detected on the gold surface are found to have molecular orbitals similar to those previously reported[15].

The thermally induced surface reaction generating fullerenes consists of a series of dehydrogenation reactions. Recently, dehydrogenation of adsorbed aromatic molecules was attributed to activation by the electronic current from the tip of a scanning tunnelling microscope[19]. To exclude such an activation mechanism and to confirm a surface-catalysed dehydrogenation process in our system, we measure the dihydrogen signal in a mass spectrometer as a function of annealing temperature. To avoid experimental artefacts due to dihydrogen desorption from the experimental apparatus, we synthesize 2,3,7,8,12,13-hexadeutero-10,15-dihydro-5*H*-diindolo[3,2-*a*:3',2'-*c*]carbazole ($C_{57}H_{27}D_6N_3$, or **1-d$_6$**), a deuterated analogue of $C_{57}H_{33}N_3$ (**1**) incorporating six deuterium atoms at strategic positions. Figure 3 shows the evolution of *m*/*z* 3 (HD) and *m*/*z* 4 (D_2) mass signals as a function of temperature. The baseline corresponds to the *m*/*z* 3 and 4 mass signals recorded when annealing the clean platinum surface (that is, before any molecular deposition) up to 750 K. The mass spectrum shows that a rapid desorption process takes place at about 700 K and should be associated with the molecular transformation shown in Fig. 2. The STM observations agree with the mass spectrometry results (Fig. 3), which indicate that there is neither modification of the molecular shape nor dehydrogenation below 400 K and that we could have partial dehydrogenation at about 500 K. STM images recorded after annealing between 400 and 600 K show asymmetrical molecules that could correspond to intermediates, that is, partially closed fullerenes that could be regarded as open-cage fullerenes[20,21].

The various experimental observations presented above provide insight into the cyclization mechanism. The observed formation of HD (*m*/*z* 3) can be attributed to the exchange of H_2 and D_2, which is known to be catalysed by platinum with an activation energy of 0.23 eV (ref. 22) and is enhanced in our system owing to the relatively high temperature of the dehydrogenation process. Therefore, hydrogen and deuterium are gathered by the platinum surface, where they diffuse, react with each other and finally desorb as H_2, HD and D_2. The platinum-induced dehydrogenation of the precursor that produces the hydrogen and deuterium atoms is facilitated by the strong interaction of the molecule with the platinum surface. According to our density functional theory calculations, this interaction distorts the molecule in such a way that the molecular wings approach the surface and enable platinum-catalysed dissociation of hydrogen atoms from the adsorbed molecule (Fig. 1b). Conversely, if the molecule does not interact strongly with the surface, as in the case of a gold (111) surface, cyclodehydrogenation does not take place. After consecutive release of the hydrogen atoms to the surface, the molecule is assumed to spontaneously cyclize. We note that although a complete density functional theory simulation of this complex process is not possible, our theoretical calculations for the $C_{60}H_{30}$ free molecule provides evidence that dehydrogenation induces a strong tendency towards cyclization. The removal of hydrogen atoms close to the central ring triggers conformational changes such that the molecular wings approach each other and a fullerene semi-cage is formed in a process that proceeds without an energy barrier. Furthermore, a thorough study of the completely dehydrogenated molecule shows that the different possible paths leading from the planar conformation to the complete fullerene cage have energy barriers less than 0.3 eV, which can be easily overcome with the thermal energy available during annealing (Supplementary Information, section 2.4).

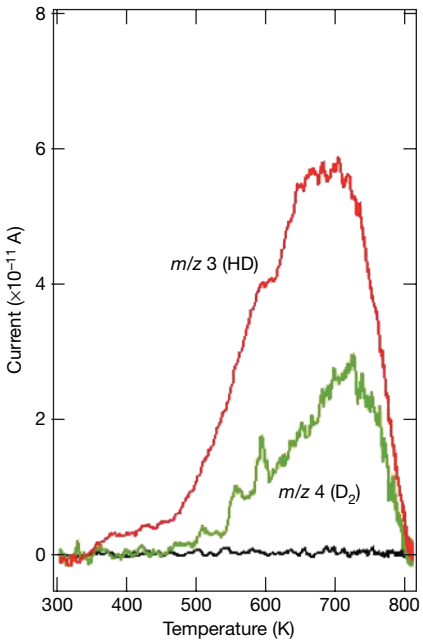

Figure 3 | TPD experiment of the cyclodehydrogenation process. Temperature evolution of the masses corresponding to HD (*m*/*z* 3) and D_2 (*m*/*z* 4), recorded after depositing $C_{57}H_{27}D_6N_3$ on the surface. Thermal desorption takes place at around 500 K. The *m*/*z* 4 signal has been scaled by a factor of eight. The black line is the result of recording the HD signal without depositing molecules on the platinum surface.

To explore the feasibility of both our controlled synthesis method outside an UHV environment and the potential for scale-up, we use platinum nanopowder instead of a single-crystal substrate. In this experiment, compound **2** is deposited from a $CHCl_3$ solution onto a large excess of platinum nanopowder and heated under vacuum (10^{-4} mbar) at 700 K for 20 min. For this sample, the laser desorption–ionization time-of-flight mass spectrum in negative-ion mode clearly shows the presence of C_{60} (Supplementary Information, section 2.6).

METHODS SUMMARY

The syntheses of $C_{60}H_{30}$ and $C_{57}H_{33}N_3$ were performed by alkylation of 10,15-dihydro-5*H*-diindeno[1,2-*a*:1',2'-*c*]fluorene (truxene) and, respectively, 10,15-dihydro-5*H*-diindolo[3,2-*a*:3',2'-*c*]carbazole (5,10,15-triazatruxene)[6–8]. Cyclization experiments have been performed *in situ* in an UHV system with a base pressure of 1×10^{-10} mbar equipped with Auger electron spectroscopy, low-energy electron diffraction optics, STM at room temperature (300 K) and TPD. The molecules were deposited *in situ* by thermal evaporation on a previously atomically cleaned platinum (111) surface. Calculations are based on density functional theory as implemented in two different total-energy pseudopotential codes: FIREBALL (ref. 9), where a local orbital basis is used to expand the electronic wavefunctions, and the plane-wave-basis approach CASTEP (ref. 10). Laser desorption–ionization time-of-flight experiments were performed using a Bruker Daltonics Autoflex mass spectrometer equipped with a nitrogen laser (337 nm). The instrument was operated in negative-ion, reflectron mode.

Full Methods and any associated references are available in the online version of the paper at www.nature.com/nature.

Received 13 July 2007; accepted 19 June 2008.

1. Scott, L. T. *et al.* A rational chemical synthesis of C_{60}. *Science* **295,** 1500–1503 (2002).
2. Hummelen, J. C., Knight, B., Pavlovich, J., González, R. & Wudl, F. Isolation of the heterofullerene $C_{59}N$ as its dimer $(C_{59}N)_2$. *Science* **269,** 1554–1556 (1995).
3. Vostrowsky, O. & Hirsch, A. Heterofullerenes. *Chem. Rev.* **106,** 5191–5207 (2006).
4. Komatsu, K., Murata, M. & Murata, Y. Encapsulation of molecular hydrogen in fullerene C_{60} by organic synthesis. *Science* **307,** 238–240 (2005).
5. Iwamatsu, S.-I. *et al.* Carbon monoxide inside an open-cage fullerene. *Angew. Chem. Int. Ed.* **45,** 5337–5340 (2006).
6. Gómez-Lor, B., de Frutos, Ó. & Echavarren, A. M. Synthesis of 'crushed fullerene' $C_{60}H_{30}$. *Chem. Commun.* 2431–2432 (1999).
7. Gómez-Lor, B. *et al.* Zipping up 'the crushed fullerene' $C_{60}H_{30}$: C_{60} by fifteen-fold, consecutive intramolecular H_2 losses. *Chem. Commun.* 370–371 (2002).
8. Gómez-Lor, B. & Echavarren, A. M. Synthesis of a triaza analogue of crushed-fullerene by intramolecular palladium catalysed arylation. *Org. Lett.* **6,** 2993–2996 (2004).
9. Jelinek, P., Wang, H., Lewis, J. P., Sankey, O. F. & Ortega, J. Multicenter approach to the exchange-correlation interactions in ab initio tight-binding methods. *Phys. Rev. B* **71,** 235101 (2005).

10. Segall, M. D. *et al.* First-principles simulation: ideas, illustrations and the CASTEP code. *J. Phys. Condens. Matter* **14,** 2717–2744 (2002).
11. Orzali, T., Petukhov, M., Sambi, M. & Tondello, E. STM study of the initial stages of C_{60} adsorption on the Pt(110)-(1×2) surface. *Appl. Surf. Sci.* **252,** 5534–5537 (2006).
12. Weckesser, J., Barth, J. V. & Kern, K. Mobility and bonding transition of C_{60} on Pd(110). *Phys. Rev. B* **64,** 161403 (2001).
13. Felici, R. *et al.* X-ray-diffraction characterization of Pt(111) surface nanopatterning induced by C_{60} adsorption. *Nature Mater.* **4,** 688–692 (2005).
14. Orzali, T. *et al.* Temperature-dependent self-assemblies of C_{60} on (1 × 2)-Pt(110): A STM/DFT investigation. *J. Phys. Chem. C* **112,** 378–390 (2008).
15. Pascual, J. I. *et al.* Seeing molecular orbitals. *Chem. Phys. Lett.* **321,** 78–82 (2000).
16. Schull, G. & Berndt, R. Orientationally ordered (7 × 7) superstructure of C_{60} on Au(111). *Phys. Rev. Lett.* **99,** 226105 (2007).
17. Hellgren, N. *et al.* Electronic structure of carbon nitride thin films studied by X-ray spectroscopy techniques. *Thin Solid Films* **471,** 19–34 (2005).
18. Soto, G. Synthesis of PtN_x films by reactive laser ablation. *Mater. Lett.* **58,** 2178–2180 (2004).
19. Lesnard, H., Bocquet, M. L. & Lorente, N. Dehydrogenation of aromatic molecules under a scanning tunnelling microscope: Pathways and inelastic spectroscopy simulations. *J. Am. Chem. Soc.* **129,** 4298–4305 (2007).
20. Rubin, Y. Ring opening reactions of fullerenes: Designed approaches to endohedral metal complexes. *Top. Curr. Chem.* **199,** 67–91 (1999).
21. Murata, Y., Murata, M. & Komatsu, K. Synthesis, structure, and properties of novel open-cage fullerenes having heteroatom(s) on the rim of the orifice. *Chem. Eur. J.* **9,** 1600–1609 (2003).
22. Gale, R. J., Salmeron, M. & Somorjai, G. A. Variation of surface-reaction probability with reactant angle of incidence molecular-beam study of asymmetry of stepped platinum crystal-surfaces for H-H bond breaking. *Phys. Rev. Lett.* **38,** 1027–1029 (1977).

Supplementary Information is linked to the online version of the paper at www.nature.com/nature.

Acknowledgements Authors acknowledge financial support from the national Spanish funding agency DGICYT-MEC (programmes MAT, CONSOLIDER and CTQ) and the ICIQ Foundation. Computer time was provided by the Spanish National Supercomputing Network at the MareNostrun (BSC) and Magerit (CESVIMA) supercomputers.

Author Contributions G.O. performed the experimental work related to the UHV system. G.B. performed the *ab initio* calculations. C.S.-S., R.C., M.F.L., C.R., F.J.P. and J.M. helped with STM-STS, TDS and XPS experiments and preliminary synchrotron radiation measurements. A.M.E and B.G.-L. designed and synthesized the planar precursors of (hetero)fullerenes. N.C. performed the mass spectrometry experiments. M.A.B. and J.O. wrote part of the calculation code and input and made preliminary calculations. The work was coordinated by B.G.-L. (chemistry), R.P. (theory) and J.A.M.-G. (experiment: UHV-STM molecular deposition, characterization and cyclization).

Author Information Reprints and permissions information is available at npg.nature.com/reprints. Correspondence and request of further information should be addressed to B.G.-L. (bgl@icmm.csic.es) or J.A.M.-G. (gago@icmm.csic.es).

METHODS

The syntheses of $C_{60}H_{30}$ and $C_{57}H_{33}N_3$ were performed by alkylation of 10,15-dihydro-5*H*-diindeno[1,2-*a*:1',2'-*c*]fluorene (truxene) and, respectively, 10,15-dihydro-5*H*-diindolo[3,2-*a*:3',2'-*c*]carbazole (5,10,15-triazatruxene) with 1-bromo-2-bromomethylnaphthalene, followed by a triple palladium-catalysed arylation as previously reported[6–8]. The synthesis of the hexadeuterated analogue $C_{57}H_{27}D_6N_3$ was performed according to the same procedure but starting from a hexadeutero-5,10,15-triazatruxene, obtained by reductive deuteriodebromination of hexabromo-5,10,15-triazatruxene with formic acid-d_2 and Et_3N.

Calculations were based on density functional theory as implemented in two different total-energy pseudopotential codes: FIREBALL[9], where a local orbital basis is used to expand the electronic wavefunctions and CASTEP[10], a plane-wave-basis approach. FIREBALL provides the balance of accuracy and efficiency needed to perform calculations with the extremely large unit cells (involving almost 400 atoms) that are required to study the adsorption of the planar fullerenes on the metal substrates. Its reliability has been checked against CASTEP results for the different free molecules.

To model the adsorption of the planar fullerene-precursors on the platinum (111) surface, we considered a 10×10 periodic slab including the molecule and three metal layers. Only the Γ point was included in the sampling of the Brillouin zone. The FIREBALL code with the local density approximation for the exchange-correlation functional was used for these calculations. All atoms in the molecule and the two upper metal layers were allowed to relax to their ground-state configuration with convergence criteria for the total energy and forces of 10^{-4} eV and 0.05 eV Å^{-1}, respectively.

UHV experiments were performed in a system that had a base pressure of 1×10^{-10} mbar, and Auger electron spectroscopy, low-energy electron diffraction, STM at room temperature and TPD techniques were used.

We prepared the clean platinum (111) surface through repeated cycles of Ar^+ bombardment and annealing at up to 1,250 K for 15 min in an O_2 atmosphere (1×10^{-5} mbar). The last annealing cycle was performed after removing the O_2 atmosphere from the chamber and keeping the total pressure at around 10^{-10} mbar. To prepare the clean gold (111) surface, we used the same methodology but annealed at 700 K without O_2 atmosphere in UHV (pressure during annealing, 4×10^{-10} mbar). To check for surface cleanness we used Auger electron spectroscopy, low-energy electron diffraction and STM techniques. Typical values for STM images were about +500 mV (on the sample) and 0.2 nA. XPS spectra were recorded in a different system equipped with a SPECS Phoibos150 electron spectrometer and a delay-line detector in the nine-segment mode, using monochromatic Al Kα radiation (1486.74 eV). The pressure in the analysis chamber was less than 5×10^{-10} mbar. High-resolution XPS spectra, such as that shown in Fig. 2, were obtained with a pass energy of 10 eV, which provided an overall energy resolution of 0.39 eV as measured at the Fermi edge of a silver reference sample.

To evaporate the organic molecules we used a homemade tantalum dispenser, which was calibrated with a thermocouple to fix the evaporation temperature accurately at 675 K. The molecular source was previously degassed without molecules up to 1,000 K in high vacuum (1×10^{-7} mbar). The $C_{60}H_{30}$, $C_{57}H_{33}N_3$, $C_{57}H_{27}D_6N_3$ and commercial C_{60} (98% purity; Sigma) molecules were degassed at 660 K in UHV (3×10^{-10} mbar) for two days to eliminate any organics used in the synthesis.

We performed the synthesis of C_{60} over platinum nanopowder by dropping a solution of **2** (0.5 mg) in $CHCl_3$ over 20 mg of activated platinum powder (approximate particle size, 100 nm; Aldrich). The solvent was evaporated under a nitrogen flow and the mixture was heated at 700 K in a Carbolite CTF/12/65/550 tube furnace with a temperature controller device for 20 min under vacuum conditions (10^{-4} mbar).